Journal of the Serbian Chemical Society
JSCS-info@shd.org.rs • www.shd.org.rs/JSCS
J. Serb. Chem. Soc. *82* (6) 695–709 (2017)
JSCS–4997
UDC 546.96–31+542.913:544.35+546.135–32+544.6.076.32
Original scientific paper

Low-temperature-synthesized RuO_2 from acidic chloride solution for the electrode coating applications

GAVRILO ŠEKULARAC[1•#], SANJA ERAKOVIĆ[1#], DUŠAN MIJIN[2#], VESNA PAVELKIĆ[1,3], JASMINA STEVANOVIĆ[1] and VLADIMIR PANIĆ[1*#]

[1]*Institute of Chemistry, Technology and Metallurgy, Department of Electrochemistry, University of Belgrade, Belgrade, Serbia,* [2]*Faculty of Technology and Metallurgy, University of Belgrade, Belgrade, Serbia and* [3]*The Railway College of Vocational Studies, Zdravka Čelara 14, Belgrade, Serbia*

(Received 29 December 2016, revised 20 March, accepted 22 March 2017)

Abstract: For the preparation of RuO_2 coatings on Ti substrate, the RuO_2 was synthesized in acidic aqueous medium by simple one-step low temperature-controlled microwave (MW) irradiation. The physical composition of synthesized solid phase was analysed through particle size distribution (PSD), whereas the coating was investigated for its capacitive response and activity in oxygen evolution reaction (OER). The oxide phase was found highly polydisperse, with overlapped fractions within rather narrow particle size range and clear tendency toward agglomeration. The smallest particles and their best resolved fractions were synthesized at the temperature just above the boiling point of the reaction medium, and quite below the chloride-to-oxide conversion temperature. Consequently, the highest OER activity was registered for RuO_2/Ti anodes prepared from this sample, with strong indication of different oxide structure, with respect to the electrodes prepared from samples synthesized at higher temperatures. However, the coatings from high temperature samples have considerably higher capacitance than those synthesized at lower temperatures. These findings can be rather correlated to the MW temperature-dependent oxide structure than to different morphology analysed through PSD.

Keywords: electrocatalytic oxide materials; hydrothermal synthesis; microwave synthesis; electrochemical impedance spectroscopy; pseudocapacitance.

INTRODUCTION

Electrochemically active noble metal oxides found their application as coatings for industrial electrodes,[1–5] due to the good electrocatalytic activity for chlor-

* Corresponding author. E-mail: panic@ihtm.bg.ac.rs
• Present address: Jožef Stefan Institute, Department of Physical and Organic Chemistry, Jamova cesta 39, Ljubljana, Slovenia.
Serbian Chemical Society member.
doi: 10.2298/JSC161229040S

ine evolution reaction (CER) and oxygen evolution reaction (OER),[6–9] but also for many other electrochemical reactions.[10–12] These oxides show also the excellent supercapacitive performances.[15–19] The main electrocatalytic coating component is RuO_2.[6,20–27] Typical procedure for the preparation of electrode oxide coatings on Ti substrate is by the thermal decomposition of the chloride salts.[6,27–30] In order to increase the oxide electrocatalytic activity, selectivity and operational stability, the variety of methods, based on the separation of the oxide synthesis and coating formation, have been applied. The aim was to establish the defined coating structure, which should be as much as possible independent from coating formation procedure itself.[31–39] Different types of hydrothermal oxide synthesis have been studied intensively, which promoted the sol–gel process due to improved coating stability in comparison to typical thermally prepared coatings.[35] However, the hydrothermal procedures have appeared rather complex and long-lasting for the application in practice. The time required for the complete conversions of chlorides to oxides of defined structure is rather long, since the temperature/pressure conditions are far from those required for controlled conversion.[35]

Microwave (MW)-assisted synthesis was proven to enhance many kinds of different processes, from organic synthesis[40] to extraction procedures.[41] It was shown[39] that suitable conditions for the extremely short hydrothermal synthesis of RuO_2 can be reached by highly controllable MW-assisted synthesis of the oxide from aqueous chloride solution. The corresponding coatings, prepared from the oxide synthesized at high pressures and MW temperatures above 200 °C, were found to be of high pseudocapacitance and activity for chlorine and oxygen evolution reaction. However, the applied MW conditions were rather extreme.

The aim of this work is to investigate the physical properties of RuO_2 synthesized at moderate MW conditions (low temperatures/pressure around boiling point of reaction medium) and consequently their influence on the electrochemical behaviour of corresponding RuO_2/Ti electrodes. The data were compared to those obtained in the investigation of MW-synthesized RuO_2 at higher temperatures.[39]

EXPERIMENTAL

Low temperature MW synthesis of RuO_2

The precursor for the preparation of RuO_2 coatings on Ti, the RuO_2 colloidal dispersion, was synthesized by the simple one-step temperature-controlled microwave (MW) irradiation, starting from aqueous $RuCl_3$ solution as described in previous work.[39] The reaction mixture (6 ml) was continuously mechanically stirred at 600 rpm inside a closed reactor (10 ml) and irradiated isothermally to 80, 120 and 150 °C in a MW oven (Monowave 300, Anton Paar, Ashland, VA, USA). The initial heating speed was set to the most rapid possible and the temperature was maintained constant for 5 min. The reaction mixture was cooled to 60 °C in the reactor and afterwards to ambient temperature. The obtained dispersions are denoted as

MW_{t80}, MW_{t120} and MW_{t150}. As a result of MW irradiation, initially brown precursor solution turned black with visible appearance of a solid phase.

Physical characterization

The reaction medium was subjected to dynamic light scattering (DLS) after the synthesis in order to analyse the solid phase presence. Laser-based particle size analyzer Zetasizer Nano ZS (Malvern Instruments, UK), operating at λ = 633 nm (produced by a He–Ne laser at scattering angle 173°) at 25±0.1 °C was employed. All samples were diluted with DI-water in volume ratio 1:100 and ultra-sonicated for 10 min before measurements.

Coating preparation

The reaction mediums, after MW irradiation at different temperatures, were used for the formation of a RuO_2 coating on Ti. The sand-blasted titanium rods (commercially pure, Krupp AG, Essen, Germany), 3 mm in diameter, were thoroughly etched in hot aqueous 18 % HCl solution for 20 min, rinsed by water, and dried at 100 °C. Before the application of the reaction medium onto Ti rods up to the height of 1 cm, the medium has been ultra-sonicated for 15 min. After deposition, the rod was dried at 120 °C for 30 min. These two steps were repeated and finally the coating was formed during the thermal treatment at 300 °C for 2 h. In the order to avoid possible detachment, the coating was deposited as rather thin layer in an amount of 0.11 mg cm^{-2}. Thus prepared RuO_2/Ti served as working electrodes in electrochemical testing.

Electrochemical measurements

The electrochemical experiments were carried out with 0.5 cm^2 working surface area in a three-electrode cell, with Pt gauze electrode and saturated calomel electrode (SCE; all potentials are expressed *vs*. SCE) as counter and reference electrodes, respectively. Cyclic voltammetry (CV) at 50 mV/s, quasi-steady-state polarization at 5 mV/s and electrochemical impedance spectroscopy (EIS) measurements (at open circuit potential) in 1 M H_2SO_4 were performed with a Biologic SP-200 potentiostat/galvanostat (Bio-Logic SAS, Claix, France) at room temperature. Polarization measurements were performed in the potential range 0.90– –1.32 V with preceding anode potentiostatic conditioning at 0.90 V for 10 min. EIS data were recorded with ac potential amplitude of 10 mV (root mean square, rms) around open circuit potential in a multi-sine mode, within frequency range of 100 kHz–5 mHz with 10 points per decade. The fitting of EIS data was performed in ZView® software (Scribner Associates Inc., Southern Pine, NC, USA) with data-modulus type of data weighting in maximum 100 iterations. The fitting is assumed acceptable if the chi-squared and weighted sum of squares were of the orders of 10^{-5} and 10^{-3}, respectively. With these fitting criteria, the relative error of the all equivalent circuit parameter values were below 10 % (the only exceptions was the value of R2 resistor for MW_{t150} sample, for which the fitting returned the error of 13 %).

RESULTS AND DISCUSSION

The changes in parameters, temperature (t_{MW}), the MW power (P) and heating rate ($(dt/d\tau)_\tau$), of the MW reactor in the early stages of synthesis are shown in Fig. 1. The data were analyzed during the time required to reach the desired isothermal condition, *i.e.*, during the early stages of MW irradiation. The time of about 1 min was required to reach the temperature plateau under characteristic heating conditions, which depend on the pre-set isothermal requirements. The

MW power was delivered continuously during *ca.* 6 s with no significant changes of temperature. When the power maxima, which considerably depend on required temperature (200, 400 and 650 W for 80, 120 and 150 °C, respectively), were reached after additional 5–6 s, the temperature started to increase with the different rate at the different pre-set temperatures. As in the case of power maxima, the peak heating rate can be reached faster if the required temperature is higher. In addition, the lower reaction temperature required finer power and heating rate tuning: there were two heating rate plateaus at 80 °C around 30 and 45 s, while the single one was seen at 120 °C around 30 s. No plateaus after heating rate peak could be observed at 150 °C. As a consequence, there was a minute overthrow of the pre-set temperature of 80 °C, as an indication of a hardly controllable heating conditions, at temperatures below boiling point of the reaction medium. It should be noted that the reactor pressure above standard conditions was registered only at the heating to 150 °C, which reached the steady-state value of 5.5 bar.

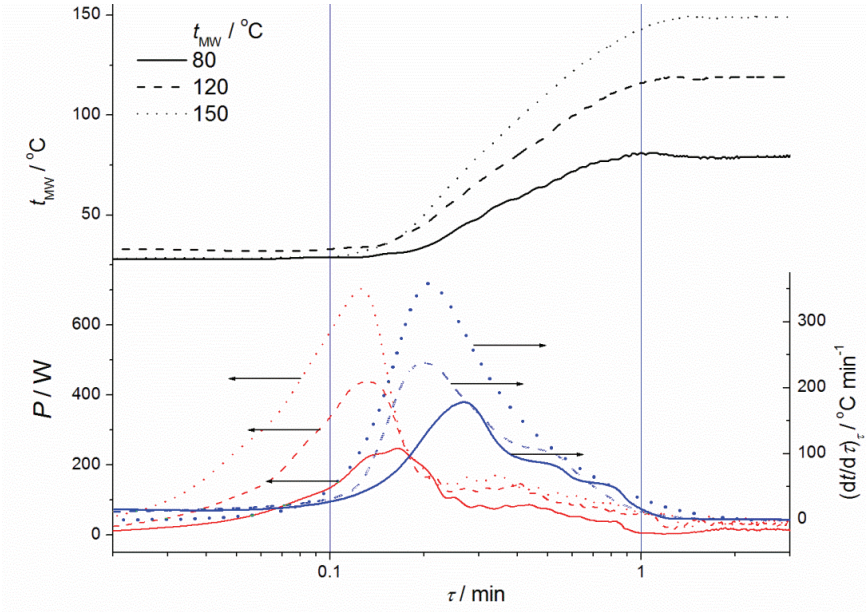

Fig. 1. The changes in MW reactor parameters: temperature (t_{MW}), MW power (P) and heating rate ($(dt/d\tau)_\tau$), in the early stages of synthesis.

The considered changes in heating parameters which precede the conditions required to maintain the steady-state heating indicated that the synthesized solid phase should be of different physical properties, since the heating was expected to affect the particle nuclei formation and subsequent particle growth. This was

checked by investigation of the particle size distribution (PSD) by the dynamic light scattering (DLS) as presented in following section.

PSD of synthesized RuO_2 solid phase

The PSDs by DLS in reaction media for RuO_2 synthesized by MW irradiation at 80, 120 and 150 °C are shown in Fig. 2. The distribution was analysed during the ten consecutive runs of light irradiation in order to check the PSD stability. All samples appeared highly polydisperse, with distinct appearance of the grains within the diameter fractions between 20 nm and 1 μm. The agglomerates of diameter above 3 μm were present in all samples, but their size distribution was becoming more pronounced upon increase in the pre-set temperature. The grains of the smallest diameter were obtained at 120 °C, grouped within well resolved fractions around 30 and 150 nm (Fig. 2B). The separation of the fractions was considerably less pronounced at lower and higher temperature (Fig. 2A and C). The initially registered peaks at higher MW temperatures (Run 1, Fig. 2B and C) were becoming better distinguished during the consecutive runs, which indicated the merging of the grains into larger ones. Consequently, in steady state Run 10 there were well resolved peaks around 50 and 300 nm for the sample synthesized at 120 °C (Fig. 2B) and around 100 and 500 nm if the synthesis temperature is increased to 150 °C (Fig. 2C). This effect was very weak, or even opposite at 80 °C (Fig. 2A). The sample at 80 °C contained the μm-sized agglomerates, stable during the runs, of extremely narrow PSD in comparison to other two samples.

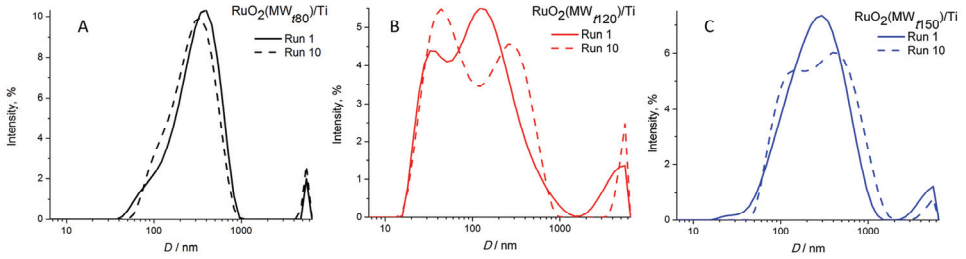

Fig. 2. Particle size distribution by intensity for RuO_2 suspension synthetized at: A) 80; B) 120 and C) 150 °C in an MW reactor. The run relates to the number of successively repeated DLS measurement.

These considerations of DLS data indicate that the pre-set temperature below the boiling point favours the particle growth formation and generates the grains of low tendency to join into agglomerates of different size. On the other hand, the intensification of the heating condition induces the nucleation and the subsequent generation of the grains, tending to form the defined grouped structures and the agglomerates of different sizes between 3 and 5 μm. This tendency of grains is reflected into the fraction of agglomerates themselves too, since they appeared

joined between first and tenth run (Fig. 2B and C) into distinct size similar to those present in sample synthesised at 80 °C (Fig. 2A). Further increase in temperature up to 220 °C did not affect the main grain fracture around 300 nm,[39] but the fractions of smaller grains (below 100 nm) was found transferred to the regions of lower diameter. These findings are a strong confirmation of nuclei formation, favoured over particle growth. Exclusively, the PSD of the sample synthesized at 200 °C did not show any presence of the agglomerates.[39] However, the particles appear to be of high surface energy, since they form stable grains and agglomerates.

The electrochemical properties of the MW-synthesized RuO_2/Ti electrodes

Electrochemical properties of RuO_2/Ti electrodes prepared from MW_{t80}, MW_{t120} and MW_{t150} samples were investigated by the cyclic voltammetry (CV), the polarization measurement and the electrochemical impedance spectroscopy (EIS). The CV curves (as specific currents per mass of the coating) are shown in Fig. 3.

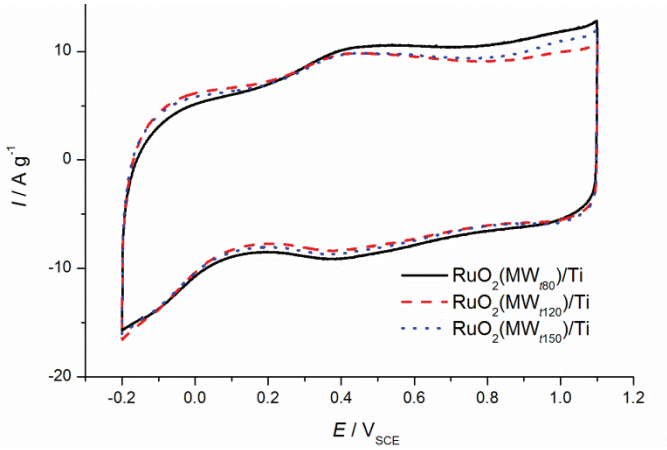

Fig. 3. The Cyclic voltammograms of RuO_2/Ti electrodes prepared from the oxide synthesized at the different temperatures. Sweep rate: 50 mV/s; electrolyte: 1 M H_2SO_4.

Cyclic voltammograms had usual shape for RuO_2/Ti electrodes obtained by the different synthesis procedures.[35] In the most of CV potential region of CV anodic branch, the highest currents were registered for $RuO_2(MW_{t80})$/Ti and the lowest for $RuO_2(MW_{t120})$/Ti electrode, although the currents were quite similar for all samples. This indicated their almost equal capacitive ability. It should be noted that the order of currents was opposite right at the beginning of charging (–0.2 to 0.1 V). This part of the anodic charging branch follows the completion of the proton insertion into the hydrous structure of the oxide in the same potential region of the cathodic branch. It appeared that the oxide synthesized at

higher temperatures was able to respond more efficiently to the redox transitions involving the lower oxidation states of Ru.[42] Similarly, the transitions related to higher Ru oxidation states were improved when the synthesis temperature was below the boiling point of the reaction ($RuO_2(MW_{t80})$/Ti). These findings indicate that the increasing temperature of MW synthesis to 120 and 150 °C produce more polycrystalline particles that create more accessible coatings with more defects sites (kink sites, defect sites, edges, etc.), which can be readily oxidized to higher oxidation states.

Total capacitance of anodes was calculated by integration of CV curves. A bit higher value was obtained for $RuO_2(MW_{t80})$/Ti, 108 F g^{-1}, in comparison to $RuO_2(MW_{t120})$/Ti and $RuO_2(MW_{t150})$/Ti, 101 and 107 F g^{-1}, respectively. In addition to small differences commented in previous paragraph, these small differences in CV capacitance could also originate from a bit more compact structure of the $RuO_2(MW_{t120})$/Ti and $RuO_2(MW_{t150})$/Ti coatings, for which more pronounced presence of a fraction of smaller particles was registered (Fig. 2).

The synthesis temperatures above 150 °C, which is assumed as optimal for good capacitive response of RuO_2,[43] caused considerable increase in CV currents.[39]

In order to investigate further coating structure-related pseudo-capacitive characteristics of synthesized RuO_2 coatings, electrochemical impedance spectroscopy (EIS) measurements at open circuit potential (OCP) were carried out. If it is assumed that OCP value corresponds to the fastest and the most convenient redox transition, the EIS analysis is expected to give more details, related to the differences in various potential regions indicated by CV curves (Fig. 3). Experimental and fitted EIS data, presented in form of complex plane and Bode plots, along with the model of applied equivalent electrical circuit (EEC), are shown in Fig. 4. The registered EIS response and the EEC structures are typical for DSAs with a well-developed TiO_2-rich interlayer.[44] The semicircle-like dependence can be seen in the high frequency range down to 400 Hz (Fig. 4B), which precedes capacitive-like response in the intermediate frequency range, down to 0.5 Hz. The semicircle is assignable to TiO_2-rich in the coating/Ti substrate interphase, created during annealing of the electrode as the product of the substrate oxidation. Its parameters found the equivalence in CPE1 and R2 EEC elements in parallel (Fig. 4A). The capacitive-like response is distributed through a transmission line generated by the elements C1-C4 and R3-R5 and is well developed as a capacitive loop, Fig. 4C. In the low frequency range, there is an indication of finite diffusion limitations to the pseudo-capacitive response, which is represented by the element CPE2. The mean values (± abs. error) of EEC parameters are shown in Fig. 5. EIS response which describes the properties of TiO_2-rich interlayer appears similar for three samples (Fig. 4A), with corresponding resistance and capacitance around 0.6 Ω and 2,5 F g^{-1}, respectively. These findings indicate that the corresponding TiO_2-rich interlayer is of similar structure since the coat-

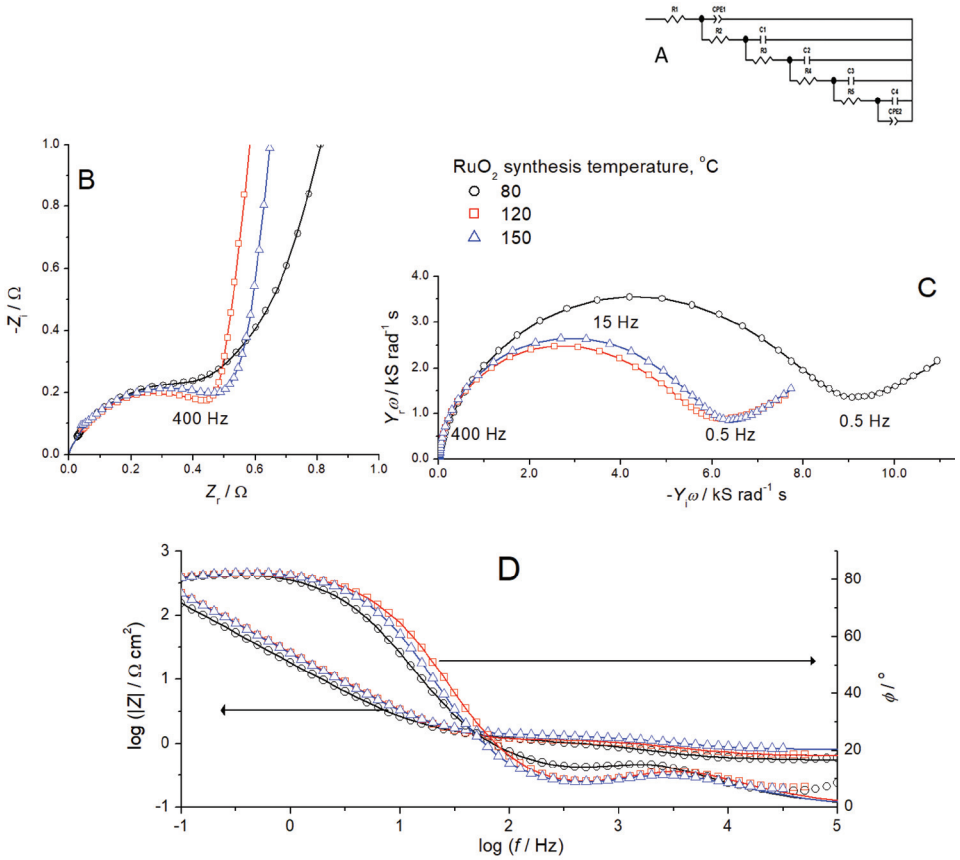

Fig. 4. The results of the fitting of measured EIS data to equivalent electrical circuit (EEC, A) presented as impedance (B) and capacitance (C) complex plane and Bode (D) plots of the RuO_2/Ti electrodes synthetized at: 80; 120 and 150 °C in an MW reactor at OCP; symbols: measured data, lines: EEC data.

ings should be of similar texture[39] created from the particles of similar size distribution around 200 nm (Fig. 2). Owing to more narrower and more stable particle distribution in case of MW_{t80}, the least compact coating structure was expected, and hence the most compact TiO_2 interlayer could be formed. This appears indicated by the larger interlayer capacitance for MW_{t80} in comparison to MW_{t120} and MW_{t150} (Fig. 4A, branch No. 1, CPE1). However, the interlayer thickness is similar for all samples and seems to be considerably thinner than the coating, since the corresponding resistance (0.6 Ω) is negligible in comparison to coating pore resistance around 100 Ω.

The capacitance complex plane plots show the difference in EIS behaviour between investigated RuO_2 coatings (Fig. 4C). Capacitive loop for $RuO_2(MW_{t80})$/Ti is larger than those obtained for $RuO_2(MW_{t120})$/Ti and $RuO_2(MW_{t150})$/Ti coatings.

The fitting of EIS response with EEC model (Fig. 4A) showed that $RuO_2(MW_{t80})$/Ti is of higher total capacitance of around 96,6 F g^{-1} in comparison to $RuO_2(MW_{t120})$/Ti and $RuO_2(MW_{t150})$/Ti coatings, which showed similar total capacitance of around 71.3 F g^{-1}. This presents more pronounced difference between $RuO_2(MW_{t80})$/Ti and other two samples, while the values are lower, with respect to CV data. This means that MW_{t80} has better pseudo-capacitive characteristics in comparison with $RuO_2(MW_{t120})$/Ti and $RuO_2(MW_{t150})$/Ti. Results obtained by fitting of experimental data are presented as capacitance and resistance through the branches of EEC, Fig. 5A and B, respectively. The more pronounced difference between the samples appears to be much higher pore resistances of $RuO_2(MW_{t120})$/Ti and $RuO_2(MW_{t150})$/Ti due to the more compact coating structure, which consequently showed the lower capacitance value in the EEC branches 3–5. As it can be seen, the capacitance values in the second branch, associated to the most outer part of the coating, are quite similar with

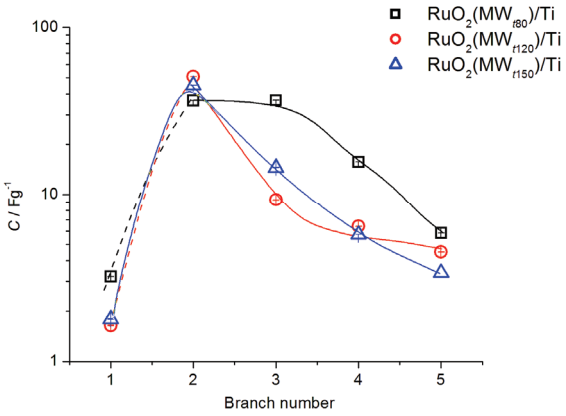

(A)

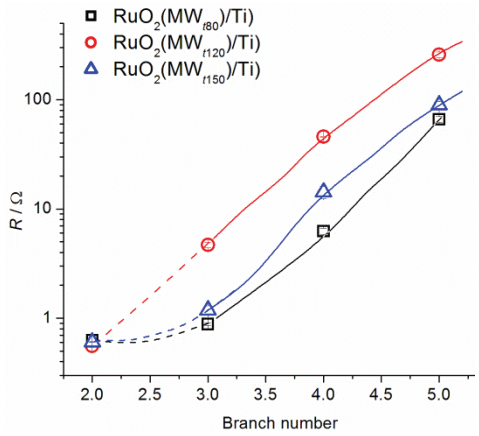

(B)

Fig. 5. A) Capacitance and B) resistance through the branches of the equivalent electrical circuit used for the fitting the impedance spectra of the RuO_2/Ti electrodes prepared from MW_{t80}, MW_{t120} and MW_{t150} samples.

even small opposite trend with respect to branches 3–5. These branches, according to the transmission line model,[45] relates to coating inner structure. Hence, higher pore resistance values were obtained for the branches 3–5. On the other hand, branch 2 presented the negligible resistance difference between samples, apparently related to the interspace of a fraction of large particles of similar size of around 200 nm for all samples. Bearing in mind that the CV data where registered with rather high potential sweep rate in comparison to EIS measurements, it could be noticed that registered CV data reflect fairly well the findings related to second EEC branches of the lower order.

It appears that the pseudo-capacitive response is sensitive to charging/discharging potential limits, with wider limits improving the capacitance performance (1.3 V in CV and only 10 mV rms amplitude in EIS), since the CV conditions double the values of those obtained by EIS. This sensitivity is less pronounced for $RuO_2(MW_{t80})$/Ti (55 % of CV capacitance is seen by EIS) than for other two samples (45 %). This indicates that more defined structure is formed at higher synthesis temperatures, with the ability to promote electrocatalytic activity (Fig. 3).

Figure 6 represents the total capacitance and total pore resistance for the samples synthesized at different MW temperatures. $RuO_2(MW_{t120})$/Ti is of largest resistance because of the compact structure created by the particles belonging to PSD fractions of the smallest diameter in comparison to other samples (Fig. 2B). Consequently the total capacitance was small, as indicated by Fig. 6. Similarly, $RuO_2(MW_{t80})$/Ti and $RuO_2(MW_{t150})$/Ti were of lower resistance with corresponding higher values of total capacitance, owing to the structure created by larger particles (Figs. 2A and C). The increase in MW temperature to 200 °C brought

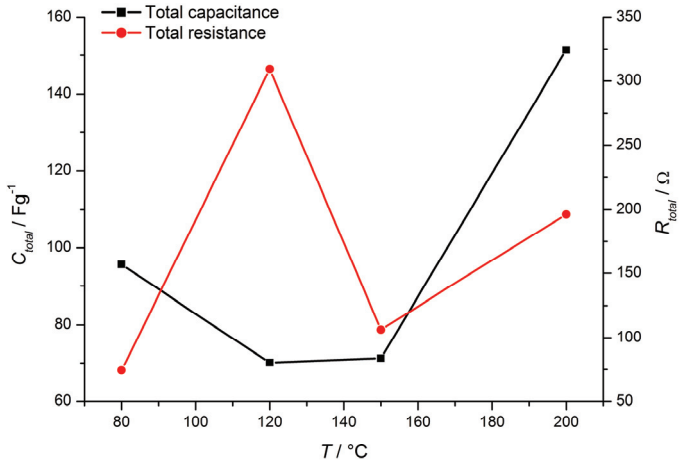

Fig. 6. Total capacitance and resistance of the RuO_2/Ti electrodes as a function of MW synthesis temperature.

about the compromise between pore resistance and coating capacitance, which resulted in highest capacitance for moderate pore resistance, but also to more defined crystalline structure as shown in previous work.[39] PSD of $RuO_2(MW_{t200})$/ /Ti[39] was consisted of similar small particle from fractions as PSDs for $RuO_2(MW_{t150})$/Ti and $RuO_2(MW_{t80})$/Ti, but with the appearance of huge agglomerates for these two samples. The intrinsic values of capacitance and resistance of $RuO_2(MW_{t200})$/Ti can also be assigned to the more uniform coating texture due to absence of the agglomerates.

Electrocatalytic properties of prepared RuO_2/Ti electrodes in oxygen evolution reaction (OER) are demonstrated by polarization curves shown in Fig. 7. Recorded polarization curves showed typical OER behaviour of RuO_2/Ti;[39,45] all of the curves show regions of the two Tafel slopes: around 40 mV below 1.23 V, and larger ones above this potential value. The region of lower Tafel slopes is typical for polycrystalline, thermally prepared RuO_2/Ti, assignable to the mechanism with indirect water oxidation over simultaneous OH/O transition as rate--determining step, mostly on (110) RuO_2. The data from previous work[39] show that the synthesis temperature just above 150 °C makes the oxide less active in this potential region. The data for 200 °C show the increase of a slope to around 55 mV and the consequent decrease in currents, Fig. 8A and B, respectively.

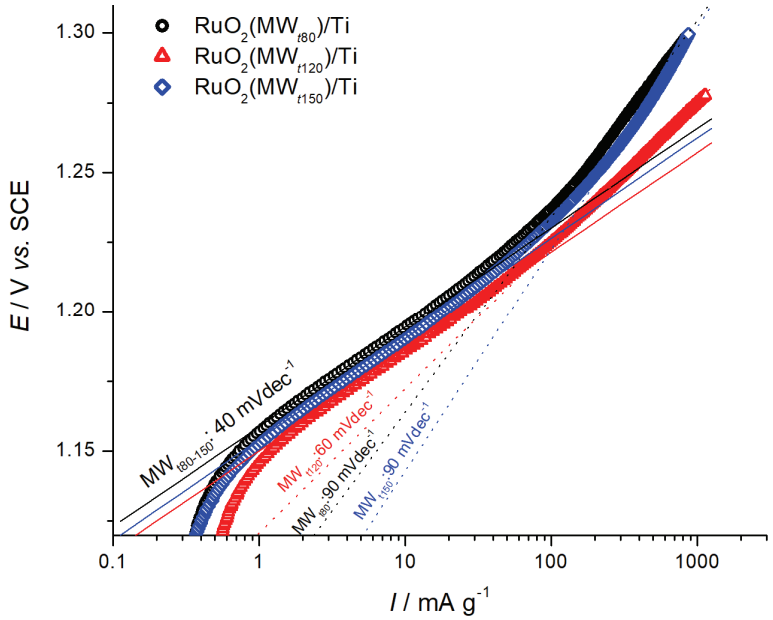

Fig. 7. Quasi-steady-state polarization curves (5 mV s^{-1}) for O_2 evolution in 1 M H_2SO_4 at room temperature on the RuO_2/Ti electrodes prepared from MW_{t80}, MW_{t120} and MW_{t150} samples.

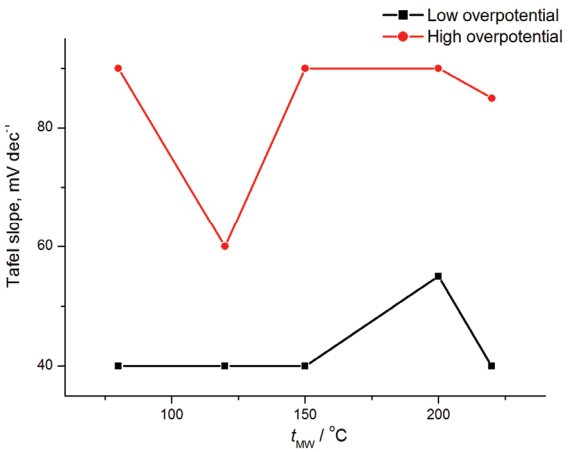

(A)

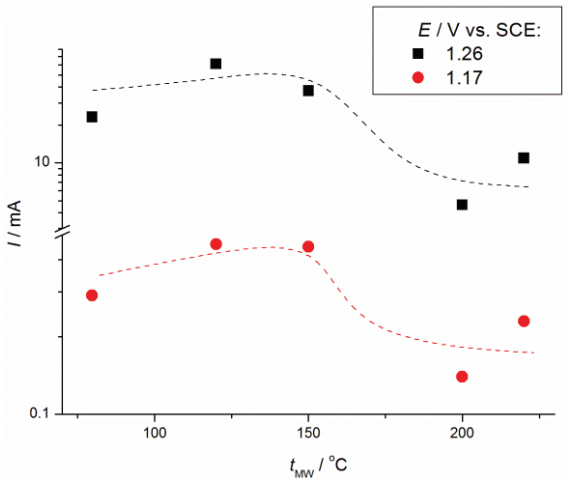

(B)

Fig. 8. A) Tafel slopes in the regions of lower and higher potentials and B) corresponding current densities at 1.26 and 1.17 V (Fig. 7) for the RuO_2/Ti electrodes as a function of RuO_2 synthesis temperature.

Further increase in temperature to 220 °C recovers the slope (the electrocatalytic features of surface active sites) and the currents only partially, with respect to low-temperature samples. This indicates that considerable changes of oxide structure take place at and above 150 °C, as reported in literature.[43] Similarly, the discontinuity is registered for large Tafel slopes, which could correspond to OER mechanism with a slowest step of direct water splitting on oxygen terminals at the oxide sites.[44] However, the temperature of discontinuity is 120 °C, which relates to considerable promotion of the electroctalytic activity. The slope is considerably lower (Fig. 8A) and corresponding currents are the highest (Fig. 8B). It follows that substantial changes in the oxide structure during the nuclei growth are initiated at the synthesis temperature above the boiling

point of the reaction mixture. It appears that MW temperature of 120 °C is able to generate a plenty of active sites at the surface of oxide particles, which is well preserved during the coating preparation and maintained as $RuO_2(MW_{t120})$/Ti unique electrocatalytic feature. It even appears that mechanism is not changed in the whole investigated potential region for $RuO_2(MW_{t120})$/Ti, and corresponds significantly to consecutive OER over OH/O transition of surface active sites.

CONCLUSIONS

RuO_2 coatings on Ti were prepared by thermal treatment of the oxide solid phase synthesized from $RuCl_3$ aqueous solution by the low temperature-controlled microwave (MW) heating. The minor difference in capacitance between coatings prepared from oxides synthesized in temperature range of 80–150 °C was registered from voltammetric responses. The difference can be associated with more compact structure of the oxide synthesized at the temperature of 120 °C in comparison to the other samples. The more compact structure was correlated to the presence of the fractions of the smallest particles. The distribution of capacitance and pore resistance, as a result of impedance measurements, showed more pronounced difference between samples due to the same cause related to coating structure. The considerable differences in capacitance and pore resistance were found in inner parts of a coating, while similar behaviour was restricted only to the outer parts, as found by voltammetric measurements.

The electrocatalytic activity of the coatings in oxygen evolution reaction (OER) was found considerably different and promoted the coatings prepared from the oxide synthesized at lower temperatures as more active. These differences were correlated to different oxide structure with characteristic structure transitions at the intrinsic temperatures just above the boiling point of reaction mixture and above the temperature recognized as crucial for optimum proton/ /electron conductivity of the oxide.

Although low synthesis temperatures were found beneficial for OER, the synthesis temperatures above 150 °C promoted the coating capacitance. This opposite finding was supposed to be due to the differences in the structure of oxide surface active sites, which appears to be generated during the MW synthesis and preserved during the formation of the coating.

Acknowledgments. Financial support for the reported investigation from the Ministry of Education, Science and Technological Development of the Republic of Serbia is acknowledged. The authors thank to Dr. Ivana Drvenica for DLS measurements.

ИЗВОД

НИСКО-ТЕМПЕРАТУРНА СИНТЕЗА RuO_2 ИЗ КИСЕЛОГ ХЛОРИДНОГ РАСТВОРА ЗА ПРИПРЕМУ ЕЛЕКТРОДНЕ ПРЕВЛАКЕ

ГАВРИЛО ШЕКУЛАРАЦ[1], САЊА ЕРАКОВИЋ[1], ДУШАН МИЈИН[2], ВЕСНА ПАВЕЛКИЋ[3], ЈАСМИНА СТЕВАНОВИЋ[1] и ВЛАДИМИР ПАНИЋ[1]

[1]Институт за хемију, технологију и металургију, Центар за електрохемију, Универзитет у Београду, Београд, [2] Технолошко–металуршки факултет, Универзитет у Београду, Београд и [3]Висока железничка школа струковних студија, Здравка Челара 14, Београд

RuO_2 је синтетисан у киселом воденом раствору једноставним микроталасним (MW) поступком у једном кораку на контролисаним ниским температурама и затим коришћен за припрему RuO_2 превлаке на подлози од титана. Синтетисана чврста фаза је окарактерисана анализом расподеле величине честица (PSD), док су капацитивност превлаке и њена активност у реакцији издвајања кисеоника (OER) испитане електрохемијским техникама. Нађено је да је оксидна фаза изражено полидисперзна, са фракцијама величине честица у уском опсегу пречника и тенденцијом ка укрупњавању. Најситније честице и изражено раздвојене фракције синтетисане су на температурама блиским температури кључања реакционе смеше, знатно испод температуре конверзије хлорида у оксид. На овим температурама је регистрована и највећа активност RuO_2/Ti аноде за OER, вероватно због различите структуре оксида у односу на узорке припремљене на вишим температурама. Међутим, нађено је да превлаке формиране од оксида синтетисаног на вишим температурама имају већу капацитивност од оних синтетисаних на нижим температрама. Овакви резултати су пре последица температурно-зависне структуре оксида, него промена у његовој морфологији које настају MW синтезом.

(Примљено 29. децембра 2016, ревидирано 20. марта, прихваћено 22. марта 2017)

REFERENCES

1. S. Trasatti, W. O'Grady, in: H. Gerisher, C.W. Tobias (Eds.), *Advances in Electrochemistry and Electrochemical Engineering*, Wiley, New York, 1981, p. 177
2. A. Cornell, F. Herlitz, in: *Proceedings of the Fourth Kurt Schwabe Corrosion Symposium*, Helsinki, Finland, 2004, p. 326
3. S. Trasatti, W. E. O'Grady, in: *Advances in Electrochemistry and Electrochemical Engineering*, Vol. 13, H. Gerischer and P. Delahay, Eds., Interscience, New York, 1980, p. 177
4. S. Horacek, S. Puschaver, *Chem. Eng. Progress* **67** (1971) 71
5. A. Nidola, in: *Electrodes of Conductive Metallic Oxides*, Part B, S. Trasatti, Ed., Elsevier, Amsterdam, 1981, p. 627
6. S. Trasatti, in: *Interfacial electrochemistry – theory, experiment and applications,* A. Wieckowski, Ed., Marcel Dekker Inc., New York, 1999, p. 769
7. De Nora elettrodi network, 2009, http://www.lidaproducts.com, accessed May, 2009
8. B.Ž. Nikolić, V.V. Panić, in *Encyclopedia of applied electrochemistry*, G. Kreysa, K-I. Ota, R. F. Savinell, Eds., Springer, New York, 2014, p. 411
9. F. Herlitz, B. Hakansson, in: *Proceedings of the Fourth Kurt Schwabe Corrosion, Symposium*, Helsinki, Finland, 2004, p. 32
10. K. Darowicki, S. Janicki, *Corr. Sci.* **41** (1999) 1165
11. S.M.A. Shibli, V.S. Gireesh, S. George, *Corr. Sci.* **46** (2004) 819
12. E. O'Sullivan, J. White, *J. Electrochem. Soc.* **136** (1989) 2576
13. C.L.P.S. Zanta, A.R. De Andrade, J.F.C. Boodts, *Electrochim. Acta* **44** (1999) 3333

14. V.V. Panić, A.B. Dekanski, T.R. Vidaković, V.B. Mišković-Stanković, B.Ž. Jovanović, B.Ž. Nikolić, *J. Solid State Electrochem.* **9** (2005) 43
15. S. Trasatti, P. Kurzweil, *Platinum Metals Rev.* **38** (1994) 46
16. B. E. Conway, *Electrochemical Supercapacitors: Scientific Fundamentals and Technological Applications*, Kluwer Academic/Plenum Publishers, New York, 1999, p. 211
17. T. Jow, J. Zheng, *J. Electrochem. Soc.* **145** (1998) 49.
18. V. Panić, T. Vidaković, S. Gojković, A. Dekanski, B. Nikolić, *Electrochim. Acta* **48** (2003) 3805.
19. I.-H. Kim, J.-H. Kim, K.-B. Kim, *Electrochem. Solid State Lett.* **8** (2005) A369.
20. J. M. Hu, J. Q. Zhang, C. N. Cao, *Int. J. Hydrogen Energy* **29** (2000) 791
21. M. H. P. Santana, L. A. De Faria, J. F. C. Boodts, *Electrochim. Acta* **49** (2004) 1925
22. C. Comninellis, P.G.J. Vercesi, *Appl. Electrochem.* **21** (1991) 335
23. M. Yagi, E. Tomita, T.J. Kuwabara, *Electroanal. Chem.* **579** (2005) 83
24. Y. W. Jung, J. Lee, Y. Tak, *Electrochem. Solid State Lett.* **7** (2004) H5
25. P. S. Patil, R. W. Kawar, S. B. Sadale, *Electrochim. Acta* **50** (2005) 2527
26. V. Jovanović, A. Dekanski, P. Despotov, B. Nikolić, R.J. Atanasoski, *Electroanal. Chem.* **339** (1992) 147
27. S. Ardizzone, S. Trasatti, *Adv. Colloid Interface Sci.* **64** (1996) 173
28. N. Yoshinaga, W. Sugimoto, Y. Takasu, *Electrochim. Acta* **54** (2008) 566
29. A. A. F. Grupioni, E. Arashiro, T. A. F. Lassali, *Electrochim. Acta* **48** (2002) 407
30. R. K. Karlsson, A. Cornell, *Chem. Rev.* **116** (2016) 2982
31. A. Marshall, B. Borresen, G. Hagen, M. Tsypkin, R. Tunold, *Mater. Chem. Phys.* **94** (2005) 226
32. A. De Oliveira-Sousa, M. A. S. Da Silva, S. A. S. Machado, L. A. Avaca, P. De Lima--Neto, *Electrochim. Acta* **45** (2000) 4467
33. P. S. Patil, R. K. Kawar, S. B. Sadale, *Appl. Surf. Sci.* **249** (2005) 367
34. M.X. Xia, C.B. Wang, Y.S. Gong, Q. Shen, L.M. Zhang, *Rare Met. Mater. Eng.* **35** (2006) 820
35. V. V. Panić, B. Ž. Nikolić, *J. Serb. Chem. Soc.* **73** (2008) 1083
36. L. Massot, P. Palau, A. Savall, P. Taxil, *J. New Mater. Electrochem. Sys.* **10** (2007) 123
37. L. Xu, Y. Xin, J. Wang, *Electrochim. Acta* **54** (2009) 1820
38. J.R. Osman, J.A. Crayston, A. Pratt, D.T. Richens, *J. Sol Gel Sci. Technol.* **46** (2008) 126
39. G. Šekularac, M. Košević, I. Drvenica, A. Dekanski, V. Panić, B. Nikolić, *J. Solid State Electrochem.* **20** (11) (2016) 3115
40. N. Božinović, B. A. Šolaja, I. M. Opsenica, *J. Serb. Chem. Soc.* **81** (11) (2016) 1225
41. A. M. Tasić, I. D. Sredović Ignjatović, Lj. M. Ignjatović, I. B. Anđelković, M. P. Antić, Lj. V. Rajaković, *J. Serb. Chem. Soc.* **81** (2016) 403
42. I. Povar, O. Spinu, *J. Electrochem. Sci. Eng.* **6** (2016) 123
43. J. P. Zheng, P. J. Cygan, T. R. Jow, *J. Electrochem. Soc.* **142** (1995) 2699
44. V. Panić, A. Dekanski, V. B. Mišković-Stanković, S. Milonjić, B. Nikolić, *J. Electroanal. Chem.* **579** (2005) 67
45. Y.-H. Fang, Z.-P. Liu, *J. Am. Chem. Soc.* **132** (2010) 18214.